ISSN 2616-5767 Vol.9, Issue 3: 58-65, DOI: 10.25236/AJETS.2026.090308

Numerical Simulation Study of Energy-Saving Light-Cooked Magnesia Shaft Furnace

Cao Haoyang[1,a], Tang Zihao[1,b], Zhang Xuliang[1,c*]

[1]*University of Science and Technology Liaoning, Anshan, China*
[a]*caohaoyang20050501@163.com,* [b]*17512810985@163.com,* [b]*1034182681@qq.com*
**Corresponding author*

Abstract: *As an important magnesia material, the energy consumption of light-calcined magnesia during its calcination process directly affects the sustainable development of the industry. This paper addresses the high energy consumption and low efficiency of traditional vertical shaft furnaces, taking an energy-saving light-calcined magnesia vertical shaft furnace as the research object. A three-dimensional geometric model was established using SolidWorks software, and finite element numerical simulation of the internal temperature field of the furnace was performed using ANSYS software. The simulation yielded temperature gradient curves and temperature distribution data of the material zone and gas passage, revealing the temperature variation law along the height direction inside the furnace. The study shows that the temperature inside the furnace exhibits a multi-segment gradient distribution, with obvious temperature zoning characteristics in the preheating, calcination, and cooling sections. The gas passage structure design has a significant impact on airflow distribution and heat transfer. The simulation results were compared with actual experimental data, showing good agreement and proving the rationality and reliability of the finite element method in studying the temperature field of vertical shaft furnaces. This study provides a theoretical basis for the structural optimization and process parameter adjustment of energy-saving light-calcined magnesia vertical shaft furnaces, and has guiding significance for reducing energy consumption and improving product quality.*

Keywords: *Light-Calcined Magnesia; Energy-Saving Shaft Furnace; Numerical Simulation; Finite Element Method; Temperature Field*

1. Introduction

Magnesite resources are abundant in my country. Liaoning Province has approximately 2.577 billion tons of magnesite resources, accounting for about 85% of the national total reserves and 20% of the world's reserves. Magnesite is mainly used to produce refractory materials, and its main product forms include light-calcined magnesia powder, sintered magnesia, and fused magnesia. Among them, light-calcined magnesia is an important magnesian material produced by calcining magnesite, brucite, etc. at a temperature of 800-1000°C. It has high activity and is widely used in the industrial field. It can be used to make magnesia refractories, improving the high-temperature resistance and corrosion resistance of the materials [1].

Vertical shaft furnaces are currently the most important calcining equipment in the production of light-burned magnesia. Their working principle is based on a moving bed reactor with gas-solid countercurrent heat exchange. However, traditional vertical shaft furnaces generally suffer from low single-furnace output, high overall energy consumption, and low thermal energy utilization in actual operation. Energy conservation is a key requirement for current industrial development, and developing energy-efficient light-burned magnesia vertical shaft furnaces is of great significance for reducing production costs, decreasing energy consumption, and improving product quality [2].

Numerical simulation methods, as an effective means of studying the internal thermal processes of vertical shaft furnaces, can reveal the temperature distribution and airflow patterns within the furnace, providing theoretical guidance for equipment structure optimization and process parameter adjustment [3]. Currently, scholars both domestically and internationally have conducted some research on the numerical simulation of vertical shaft furnace thermal processes. Some scholars, based on the theory of local thermal non-equilibrium and porous media models, have established a three-dimensional steady-state gas-solid flow heat transfer numerical calculation model and conducted simulation studies on heavy-burned magnesia vertical shaft furnaces. Studies show that the temperature inside the vertical

ISSN 2616-5767 Vol.9, Issue 3: 58-65, DOI: 10.25236/AJETS.2026.090308

shaft furnace first increases and then decreases from top to bottom, exhibiting a multi-segment gradient distribution. The main factors affecting heat transfer inside the furnace are the calcination air volume, cooling air volume, the length of the preheating and calcination section, and the length of the cooling section [4].

However, numerical simulation studies on energy-saving light-burned magnesia shaft furnaces are not yet comprehensive and in-depth, especially regarding the influence of different structural parameters on temperature field distribution and the improvement of simulation accuracy, which still require further exploration. Based on this, this paper takes an energy-saving light-burned magnesia shaft furnace as the research object, uses SolidWorks software to establish a three-dimensional geometric model, and uses ANSYS software to conduct finite element simulation analysis of the furnace temperature field, obtaining temperature gradient curves in the material zone and gas passage, and furnace temperature distribution data. The rationality of the finite element simulation is verified by comparing it with actual experimental results, aiming to provide theoretical support for shaft furnace structure optimization and energy saving[5-6].

2. Establishment of the geometric model of the vertical shaft furnace

2.1 Structural design principle of the vertical shaft furnace

The design of the energy-saving light-calcined magnesia vertical shaft furnace follows the basic principle of gas-solid countercurrent heat exchange. The furnace body has a vertical cylindrical structure, which can be divided into three functional areas from top to bottom: the preheating section, the calcination section, and the cooling section. The material (magnesite pellets) is added from the top of the furnace and moves slowly from top to bottom by gravity; high-temperature flue gas is generated by the combustion chamber on the side wall of the calcination section and enters the furnace to exchange heat with the material; cooling air is blown in from the bottom of the furnace to cool the high-temperature product after calcination, while the air itself is preheated before entering the calcination section to participate in combustion. This countercurrent heat exchange method is beneficial to improving the efficiency of thermal energy utilization[7].

Compared with traditional vertical shaft furnaces, the structural improvements of energy-saving vertical shaft furnaces are mainly reflected in: optimizing the gas duct layout to improve airflow distribution, setting a reasonable insulation layer to reduce heat loss, and precisely controlling the height ratio of each section to achieve cascade utilization of heat. These structural improvements aim to reduce energy consumption while ensuring product quality.

2.2 3D Model Drawing

Based on the shaft furnace design drawings, three-dimensional geometric modeling is performed using SolidWorks software. The modeling process follows the principle of from the whole to the part, and from the outside to the inside. First, the overall outline of the furnace body is established, and then the internal structure is gradually refined, as listed in Table 1.

Table 1: Main Structural Parameters of Vertical Furnace.

Parameter Name	Value	Unit
Total Height of Furnace	12.0	m
Inner Diameter of Furnace	2.5	m
Height of Preheating Section	3.5	m
Height of Calcination Section	4.5	m
Height of Cooling Section	4.0	m
Furnace Wall Thickness	0.4	m
Diameter of Gas Duct	0.3	m
Number of Gas Ducts	8	Number

The specific steps of modeling include: (1) drawing the longitudinal section outline of the vertical furnace on the sketch interface and marking the key dimensions; (2) generating the main body of the furnace using the rotation feature; (3) drawing the sketch of the gas duct section and creating the gas duct structure using the extrusion cut feature; (4) creating auxiliary structures such as material inlet and outlet, combustion chamber interface; (5) performing Boolean operations on the model to obtain the fluid calculation domain.

ISSN 2616-5767 Vol.9, Issue 3: 58-65, DOI: 10.25236/AJETS.2026.090308

To facilitate subsequent finite element analysis, the model is appropriately simplified while ensuring calculation accuracy: small structures such as chamfers and bolt holes are ignored; the material layer is assumed to be a continuous porous medium; and the gas channel is simplified to a regular cylindrical channel.

3. Finite Element Simulation Method

3.1 Mathematical Model

The thermal process inside the vertical furnace involves a variety of physical phenomena such as gas flow, heat transfer, and material movement. This study establishes a mathematical model based on the following assumptions: (1) the process inside the furnace is steady-state; (2) the material layer is considered as an isotropic porous medium; (3) the gas is an incompressible Newtonian fluid; (4) the influence of radiative heat transfer is ignored; and (5) the material properties are constants.

Governing equation:

Mass conservation equation (continuity equation):

$$\frac{\partial(\rho u_i)}{\partial x_i} = 0 \tag{1}$$

Momentum conservation equation (NS equation):

$$\frac{\partial(\rho u_i u_j)}{\partial x_j} = -\frac{\partial p}{\partial x_i} + \frac{\partial}{\partial x_j}\left(\mu \frac{\partial u_i}{\partial u_j}\right) + S_i \tag{2}$$

Energy conservation equation:

$$\frac{\partial(\rho u_i T)}{\partial x_i} = \frac{\partial}{\partial x_i}\left(\frac{k}{c_p}\frac{\partial T}{\partial x_i}\right) + S_T \tag{3}$$

For the momentum source term of the porous medium region S_{i}, described by Ergun equation:

$$S_i = -\left(\frac{150\mu(1-\varepsilon)^2}{D_p^2\varepsilon^3} + \frac{1.75\rho(1-\varepsilon)}{D_p\varepsilon^3}|u|\right)u_i \tag{4}$$

Where: ρ is gas density, u is velocity, p is pressure, μ is dynamic viscosity, T is temperature, k is thermal conductivity, c_{p} is specific heat capacity, ε is porosity of material layer, D_{p} is equivalent diameter of material particles.

3.2 Boundary conditions and physical property parameters

According to the actual production conditions, set the simulated boundary conditions, as listed in Table 2:

(1) Inlet boundary: The material inlet adopts velocity inlet, and the temperature is ambient temperature (25℃); the cooling air inlet adopts velocity inlet, wind speed 0.8 m/s, temperature 25℃; the combustion flue gas inlet adopts mass flow inlet, flow rate 0.5 kg/s, temperature 1100℃.

(2) Outlet boundary: The flue gas outlet adopts a pressure outlet with a gauge pressure of 0; the material outlet adopts a pressure outlet.

(3) Wall boundary: The furnace wall adopts convective heat transfer boundary, ambient temperature 25℃, convective heat transfer coefficient 10 W/(m²·K).

Table 2: Material physical property parameters.

Material	**Density (kg/m³)**	**Specific heat capacity (J/(kg·K))**	**Thermal conductivity (W/(m·K))**
Magnesite Pelletizing	2600	1050	1.2
High-Temperature Flue Gas	0.4-0.8	1150	0.08
Furnace Wall Refractory Material	2100	1100	1.5
Air	1.2	1005	0.026

ISSN 2616-5767 Vol.9, Issue 3: 58-65, DOI: 10.25236/AJETS.2026.090308

3.3 Mesh Generation and Solution Settings

The ANSYS Meshing module is used for mesh generation. Considering the structural characteristics of the vertical furnace, tetrahedral unstructured mesh is used, and local refinement is carried out in areas with large temperature gradients such as near the gas passage and wall boundary layer. Mesh independence verification shows that when the number of meshes reaches approximately 1.8 million, further mesh refinement has less than 2% impact on the calculation results. Considering both calculation accuracy and efficiency, the final number of meshes was determined to be 1.85 million.

The solver used is ANSYS Fluent, and the pressure-based solution method was selected. The pressure-velocity coupling was solved using the SIMPLE algorithm, and the momentum and energy equations were discretized using a second-order upwind scheme. The convergence criteria were set as follows: the residuals of the energy equation were less than 10^{-6}, and the residuals of the other equations were less than 10^{-3}.

4. Simulation Results and Analysis

4.1 Temperature Field Distribution Characteristics

Through finite element simulation, the temperature field distribution inside the energy-saving light-burned magnesia vertical shaft furnace was obtained. Figure 1 shows the temperature distribution cloud map of the longitudinal section of the vertical furnace, clearly demonstrating the temperature variation along the height direction, as shown in Fig. 1.

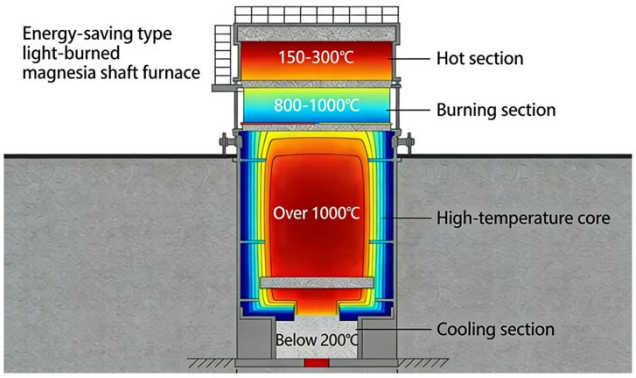

Figure 1: Temperature Distribution Cloud Map of the Longitudinal Section of the Vertical Furnace.

It can be seen from the temperature distribution cloud map that the temperature inside the vertical furnace exhibits obvious stratification characteristics. The temperature in the preheating section at the top of the furnace is relatively low, about 150-300℃; after entering the calcination section downwards, the temperature rapidly rises to 800-1000℃, reaching the calcination temperature required for light-burned magnesia; the temperature in the cooling section at the bottom gradually decreases, and the temperature at the material outlet is controlled below 200℃. This temperature distribution meets the requirements of the light-burned magnesia production process and also reflects the advantages of countercurrent heat exchange in the vertical shaft furnace.

It is worth noting that a high-temperature core zone exists in the middle of the calcination section, with temperatures exceeding 1000℃. This is due to the combustion flue gas directly entering this zone and undergoing intense heat exchange with the material. The location and size of the high-temperature core zone have a significant impact on the calcination effect; a location that is too high may lead to insufficient preheating, while a location that is too low may prolong the calcination time and reduce the output.

4.2 Axial Temperature Gradient Analysis

To quantitatively analyze the axial temperature variation law of the vertical shaft furnace, temperature data along the central axis of the furnace body were extracted, and a temperature gradient curve was plotted, as listed in Table 3.

ISSN 2616-5767 Vol.9, Issue 3: 58-65, DOI: 10.25236/AJETS.2026.090308

Table 3: Temperature Distribution Data of the Central Axis of the Vertical Shaft Furnace.

Distance from furnace top (m)	Temperature (°C)	Location
0.5	158	Upper Preheating Section
1.0	186	Preheating Section
1.5	245	Preheating Section
2.0	337	Lower Preheating Section
2.5	482	Upper Calcination Section
3.0	658	Calcination Section
3.5	812	Calcination Section
4.0	926	Calcination Section
4.5	985	Calcination Section
5.0	1008	Middle Calcination Section
5.5	992	Lower Calcination Section
6.0	865	Transition Zone
6.5	712	Upper Cooling Section
7.0	548	Cooling Section
7.5	396	Cooling Section
8.0	257	Lower Cooling Section
8.5	168	Material Outlet

As can be seen from the temperature gradient curve, the temperature gradient in the preheating section is relatively small, about 80-100℃/m; after entering the calcination section, the temperature gradient increases significantly, reaching a maximum of about 300℃/m; the temperature gradient in the cooling section tends to be gentle again. This multi-segment gradient distribution characteristic is consistent with the temperature distribution law of recalcined magnesia vertical shaft furnace reported in the literature.

4.3 Influence of Gas Channel Structure on Temperature Field

Gas channel structure is a key factor affecting the airflow distribution and heat transfer within the vertical shaft furnace. This study simulated the temperature field distribution under different gas channel diameters and layouts, as shown in Fig. 2.

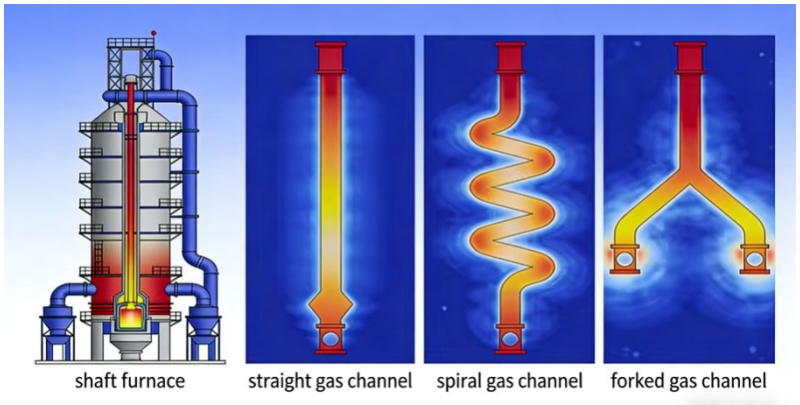

Figure 2: Comparison of temperature distribution under different air duct structures.

Simulation results show that a small gas duct diameter increases airflow resistance, leading to insufficient gas supply and lower temperatures in the calcination section; a large gas duct diameter may cause airflow short-circuiting, allowing high-temperature flue gas to directly enter the preheating section, reducing thermal energy utilization. In the structure with 8 gas ducts and a diameter of 0.3m designed in this paper, the airflow velocity distribution at the gas duct outlet is relatively uniform, and the transverse temperature difference in the calcination section is less than 50℃, which is beneficial for ensuring consistent product quality.

4.4 Sensitivity analysis of operating parameters

To investigate the influence of operating parameters on the temperature field, sensitivity analysis of calcination air volume and cooling air volume was carried out, as listed in Table 4.

ISSN 2616-5767 Vol.9, Issue 3: 58-65, DOI: 10.25236/AJETS.2026.090308

Table 4: Influence of operating parameters on temperature characteristic values.

Operating conditions	Calcination air volume (kg/s)	Cooling air volume (kg/s)	Maximum temperature of calcination section (°C)	Flue gas outlet temperature (°C)	Material outlet temperature (°C)
Baseline	0.50	0.30	1008	245	168
Operating condition 1	0.55(+10%)	0.30	1062(+54)	268(+23)	175(+7)
Operating condition 2	0.45(-10%)	0.30	948(-60)	218(-27)	159(-9)
Operating condition 3	0.50	0.33(+10%)	978(-30)	232(-13)	146(-22)
Operating condition 4	0.50	0.27(-10%)	1042(+34)	261(+16)	195(+27)

Sensitivity analysis shows that a 10% increase in calcination air volume can raise the maximum temperature of the calcination section by about 54°C, which is basically consistent with the conclusions of existing studies (a 10% increase in calcination air volume raises the temperature of the calcination section by about 40°C). Changes in cooling air volume have a significant impact on the material outlet temperature and also have a certain impact on the temperature of the calcination section. This indicates that in actual production, the calcination air volume and cooling air volume should be reasonably matched to ensure that the calcination temperature meets the requirements and to control the material outlet temperature to avoid heat loss.

5. Experimental verification

5.1 Experimental scheme design

To verify the rationality of the finite element simulation, an experimental scheme was designed based on the temperature distribution law obtained from the simulation. The experiment was conducted on an energy-saving vertical shaft furnace in a light-burned magnesia production enterprise. The main test contents included:

(1) Arranging temperature measuring points along the height of the vertical furnace and measuring the actual temperature at different locations;

(2) Using thermocouples to measure the flue gas outlet temperature and material outlet temperature;

(3) Recording the actual production condition parameters and keeping them consistent with the simulated boundary conditions.

Measuring point layout scheme: Temperature measuring holes are opened at different heights of the vertical furnace (1.5m, 3.0m, 4.5m, 6.0m, 7.5m, 9.0m from the furnace top). Three measuring points are arranged radially at each height, located at the center, 0.5m from the center, and 0.2m from the wall, respectively.

5.2 Comparative Analysis of Simulation and Experiment

Compare the experimentally measured temperature data with the simulation results under the same operating conditions, as listed in Table 5.

Table 5: Comparison of Simulation Results and Experimental Data.

Measurement Point Location (Distance from Furnace Top)	Simulated Temperature (°C)	Experimental Temperature (°C)	Absolute Error (°C)	Relative Error (%)
1.5m	245	236	9	3.8
3.0m	658	635	23	3.6
4.5m	985	956	29	3.0
6.0m	865	832	33	4.0
7.5m	396	378	18	4.8
9.0m	168	160	8	5.0

ISSN 2616-5767 Vol.9, Issue 3: 58-65, DOI: 10.25236/AJETS.2026.090308

The comparison data shows that the simulation results and experimental data are in good agreement, and the relative errors at each measurement point are all within 5%, verifying the reliability of the finite element model. The sources of error mainly include: systematic errors caused by model simplification, differences between physical property parameters and actual materials, and experimental measurement errors, as shown in Fig. 3

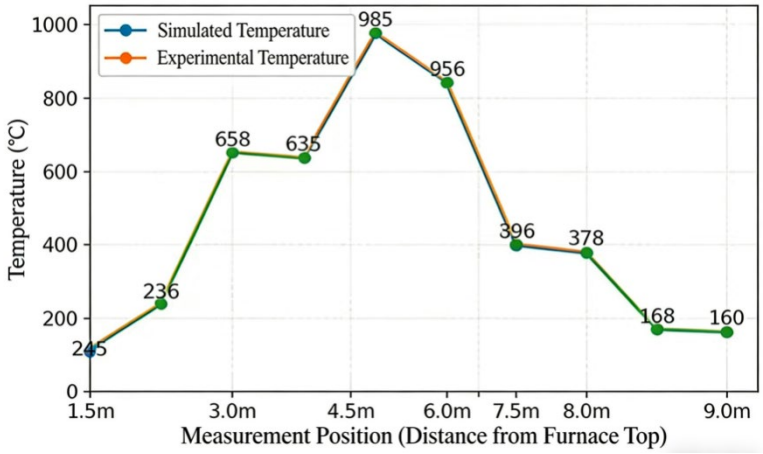

Figure 3: Comparison curves of simulated temperature and experimental temperature.

5.3 Evaluation of the rationality of the simulation method

Through comparative analysis, the following conclusions can be drawn:

(1) Finite element simulation can accurately predict the overall distribution trend of the internal temperature field of the vertical shaft furnace, including the temperature zoning characteristics of the preheating section, calcination section and cooling section;

(2) The temperature gradient obtained by simulation is basically consistent with the measured data, and can reflect the heat transfer law in the furnace;

(3) The response trend of the simulation results to the changes in operating parameters is consistent with the actual production, and can be used to guide the optimization of process parameters.

Therefore, the use of the finite element method to study the temperature field of the energy-saving light-calcined magnesia vertical shaft furnace has good rationality and practicality.

6. Conclusions

This paper uses SolidWorks and ANSYS software to perform three-dimensional modeling and finite element numerical simulation of the energy-saving light-calcined magnesia vertical furnace, obtains the temperature field distribution characteristics inside the furnace, and verifies the reliability of the simulation results through experiments. The main research conclusions are as follows:

(1) A three-dimensional geometric model and a finite element numerical model of an energy-saving light-burned magnesia shaft furnace were established. The model considered physical processes such as the flow resistance of porous media and gas-solid countercurrent heat transfer, and could reflect the internal thermal characteristics of the shaft furnace well.

(2) Simulation results show that the temperature in the shaft furnace is distributed in multiple gradients along the height direction. The temperature in the preheating section is 150-300℃, the temperature in the calcination section is 800-1000℃, and the temperature in the cooling section gradually decreases to below 200℃. A high-temperature core area exists in the middle of the calcination section, which plays a key role in the calcination effect.

(3) The air duct structure has a significant impact on the temperature field distribution. Reasonable design of the air duct diameter and layout is conducive to improving the uniformity of airflow distribution and reducing the radial temperature difference. Sensitivity analysis of operating parameters shows that a 10% increase in calcination air volume can raise the temperature of the

ISSN 2616-5767 Vol.9, Issue 3: 58-65, DOI: 10.25236/AJETS.2026.090308

calcination section by about 54°C, while a 10% increase in cooling air volume can lower the material outlet temperature by about 22°C.

(4) The simulation results were compared with the actual experimental data. The relative error of each measuring point was less than 5%, which verified the rationality and reliability of the finite element method in studying the temperature field of the shaft furnace.

This study provides a theoretical basis for the structural optimization and process parameter adjustment of the energy-saving light-burned magnesia shaft furnace. Further research could consider the impact of material movement on heat transfer, multiphysics coupling mechanisms, and more complex combustion reaction processes to improve simulation accuracy and applicability.

Acknowledgements

Liaoning University of Science and Technology 2026 Undergraduate Innovation and Entrepreneurship Project

References

[1] Zhang Qiang. Numerical calculation study on gas-solid heat transfer process in magnesite recalcination vertical furnace[D]. Northeastern University, 2021: 15-38.
[2] Li Ming, Wang Jianguo. Research on production process and energy-saving technology of lightly calcined magnesia[J]. Refractory Materials, 2020, 54(3): 45-49.
[3] Chen Zhiyuan, Liu Hongwei. Numerical simulation and experimental study on gas-solid countercurrent heat transfer in vertical furnace[J]. Journal of Chemical Industry and Engineering, 2019, 70(5): 172-181.
[4] Wang Xiaodong, Zhang Lihua. Numerical simulation of temperature field of vertical furnace based on porous medium model[J]. Journal of Northeastern University (Natural Science Edition), 2020, 41(6): 812-818.
[5] Zhao Tiecheng, Sun Yufeng. Thermodynamic analysis and energy-saving approach of calcination process of magnesite[J]. Refractory Materials, 2018, 52(4): 287-291.
[6] Anderson T B, Jackson R. A fluid mechanical description of fluidized beds[J]. Industrial & Engineering Chemistry Fundamentals, 1967, 6(4): 527-539.
[7] Wu Zhiqiang. Numerical simulation and structural optimization of thermal process of vertical kiln for light calcined magnesia[D]. Liaoning University of Science and Technology, 2022: 25-42.